Journal of Structural Engineering & Applied Mechanics (2022) 5(4):289-299
DOI 10.31462/jseam.2022.04289299

RESEARCH ARTICLE

Experimental and numerical determination of interlayer shear strength of glass fiber-reinforced epoxy composites

Mustafa Albayrak[1*], Ahmet Murat Asan[2], Mete Onur Kaman[2], İlyas Bozkurt[3]

[1] Inonu University, Department of Machine and Metallurgy Technologies, Malatya, Turkey
[2] Firat University, Mechanical Engineering Department, Elazıg, Turkey
[3] Muş Alparslan University, Mechanical Engineering Department, Elazıg, Turkey

Article History

Received 19 October 2022
Accepted 21 November 2022

Keywords

Glass fiber composites
Progressive failure analysis
Short beam test
LS-DYNA

Abstract

This study aims to produce glass fiber composite plates by vacuum infusion method and to determine the interlaminar shear strength (ILSS) under the short beam test. For this purpose, composite plates were produced under the effect of vacuum and temperature by adding glass fiber layers on a flat vacuum table. Short beam tests were carried out on the obtained laminated composite plates and the interlayer shear strength, which is generally characterized by delamination damage, was investigated. In the numerical part, the tests were modeled using the LS-DYNA finite element package program, and the Hashin damage criterion-based material model was used to see the damages that occurred in the composite structure after the tests.

1. Introduction

Along with the developments in technology, the innovation and application of composite materials are seen as a turning point in modern industry. Fiber-reinforced composites can be manufactured in plate form (thin section) due to their high mechanical properties. Fiber-reinforced composites are materials that exhibit brittle fracture behavior and can be subjected to different static and dynamic loads when their application areas are considered. Under these loads, damage to the structure occurs due to matrix cracks and fiber breaks. These fractures also cause the initiation and progression of damage on surfaces outside the contact zone under load, and sometimes even invisible delamination damage. Delamination is a critical failure mechanism in composite laminates, often characterized by interlayer shear strength [1], and this strength value is one of the most important parameters in determining a composite's ability to resist delamination damage. Therefore, accurate estimation of this value is important for composites. Sritharan and Askari [2] used helical carbon nanotubes with various weight percentages as additional reinforcement to glass fiber composite laminates. They calculated the short-beam strength of the reinforced composites they obtained according to the ASTM D2344 standard. Allot and Czabaj [3] performed short beam tests according to ASTM D2344 standards to measure the interlayer shear strength (ILSS) of polymer matrix composites (PMCs). The effect of sample size on damage mode and interlaminar shear strength was investigated. Tretiak et al [4] performed short beam tests using a reduced cross-sectional area approach to estimate the short beam shear strength of

* Corresponding author (mustafaalbayrak@inonu.edu.tr)

eISSN 2630-5763

carbon/epoxy laminates. They used the reduced cross-sectional area to estimate the short beam shear strength of laminates containing voids. Demiral et al. [5] investigated the interplay damage behavior of glass fiber composites with microvascular channels. Short beam bending tests and finite element analyzes were performed according to ASTM D2344 for two stacking configurations, [90/0]3s and [0/90]3s. Kumar et al. [6] designed different surface modifications with aluminum-carbon composite sandwich panels. Then, they obtained the effect of this surface modification on shear strength between layers by applying a shear beam test for samples with different aperture/depth ratios. Kotik and Ipiña [7] compared the effect of Unifilo layers on glass fiber-reinforced composite laminates under interlayer shear stresses under static and fatigue conditions using the short beam test. Xin et al. [8] have produced short and short continuous fiber synergistic reinforced composites by the production of fused filaments. Then, the effects of short fiber content on filament bonding properties were evaluated by performing short beam tests and in-plane tensile shear tests. Dinesh and Gowthaman [9] applied a short beam test on the samples obtained by producing plain and ZnO nanowire-reinforced unidirectional glass/epoxy composites.

When the studies are examined, short beam tests were carried out on glass [1], carbon [10], and hybrid [11] composites, and it was observed that the effects of fiber reinforcement elements on shear strength between layers were studied experimentally. However, unlike the literature in this study, unlike the literature; Glass fiber composites were produced and interlayer shear strength and modulus were determined experimentally and numerically according to ASTM D2344 standards. In the numerical study, progressive damage analysis of glass fiber composites was performed in three dimensions. The fiber shrinkage, crushing, and crack damages obtained as a result of the analysis are presented in comparison with the experimental results.

2. Experimental details

2.1. Materials and manufacturing

To determine the shear strength between layers, flat composite plates with 5mm thickness and 150×300mm dimensions were designed and produced. The samples obtained were 18 layers and were arranged in one direction. Glass fiber woven fabrics with twill 2×2 weave type were added to the vacuum infusion table and production was carried out by impregnating with epoxy under vacuum. The production of glass fiber reinforced composites by vacuum infusion method is shown in Fig. 1 and the sample obtained after production is shown in Fig. 2. Also in Fig. 2, the composite plate produced, the test sample prepared according to ASTM D2344 standards, and the boundary conditions are given.

A mixture of LR160 resin and LH160 hardener at a ratio of 100/20 by weight, together with braided glass fiber with 300 gr/m2 areal density, was used in production. After the homogeneous mixture obtained was impregnated with glass fiber fabrics under vacuum, it was cured at 100°C for 2 hours. Afterward, the temperature unit was turned off and the samples under vacuum were kept at room temperature for 24 hours. The samples obtained at the end of this period were cleaned and stacked. Three test specimens were prepared by cutting the flat composite plates produced according to ASTM D2344 standards with a thickness of h=5mm, a length of L = 50 mm, and a width of W = 10mm. Afterward, the samples were made ready for testing by placing them between two 4 mm diameter fixed support rollers and a 10 mm diameter movable loading roller as shown in Fig. 3. Here, the beam span length $L_s = 6h$ = 30 mm is determined according to ASTM D2344 standards.

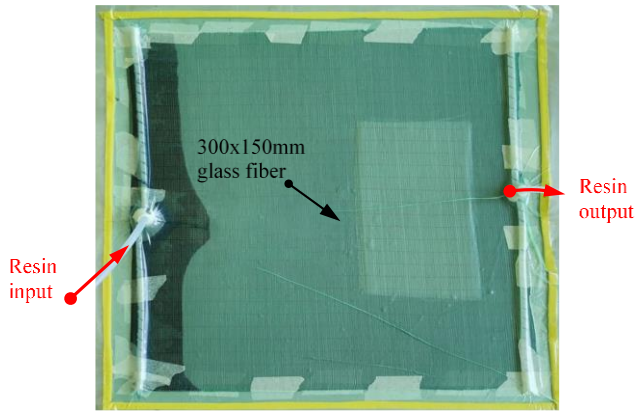

Fig. 1. Composite plate production by the vacuum infusion method

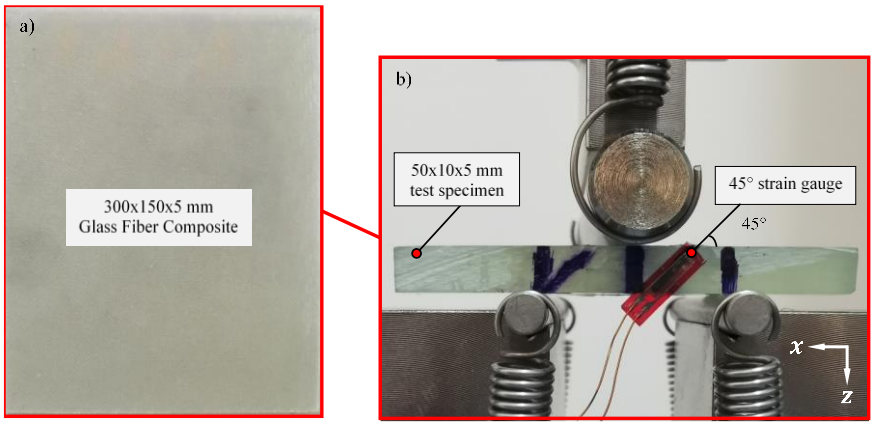

Fig. 2. a) Composite plate, b) Specimen

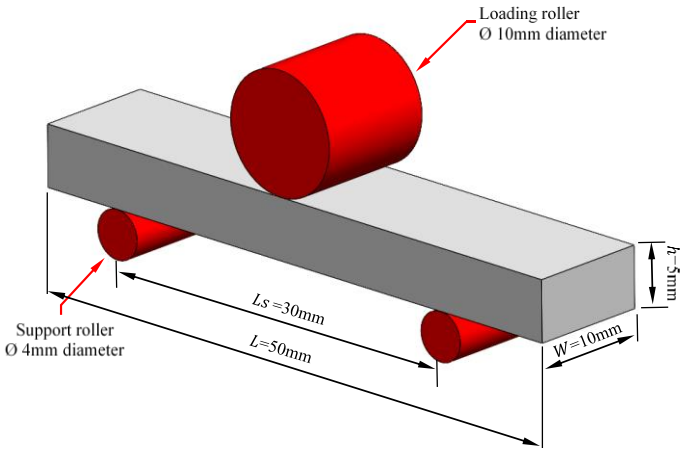

Fig. 3. Configuration of the ASTM D2344

2.2. Short beam test

Short beam tests were carried out on the Shımadzu AGS-X tester with 10 kN capacity. The cross-head used in the experiment has a cylindrical geometry, and a diameter of 10 mm. The head velocity was set to 1 mm/min during the test period. As a result of the experiments, reaction force-displacement, reaction force time, and shear stress-shear strain graphs were obtained. To determine the out-plane shear moduli G_{xz} with 10 mm width, 50 mm length, and 5 mm thickness were manufactured by using the standard Test Method for Short-Beam Strength as described in ASTM D2344. The strain-gage was glued along the natural axis of the longitudinal lateral surface of the specimen at the angle of 45° with a transverse direction as shown in Fig. 2 (In-plane $x-z$ for G_{xz}). Maximum shear stresses in the natural axis were calculated as given in Eq. (1). G_{xz} can be calculated by using Eqs. (2) and (3).

$$\tau_{xz} = \frac{3}{4}\frac{P_{max}}{Wh} \tag{1}$$

where P_{max} is the damage load, W is the sample width and h is the sample thickness. This relation is based on the theoretical maximum shear stress achieved in classical Timoshenko engineering beam theory [12]. ε is the strain rate read from the strain gauge as in the following.

$$\gamma_{xz} = 2\varepsilon \tag{2}$$

$$G_{xz} = \frac{\tau_{xz}}{\gamma_{xz}} \tag{3}$$

3. Numerical method

3.1. Geometrical model

Short beam test analyses were carried out in the LS-DYNA finite element program. An 8-node solid element type was used in the modeling of composite plates. To obtain realistic boundary conditions, instead of fixing the boundary nodes, loading and support rollers are modeled. The loading and support rollers were defined as rigid. The support rollers are fixed in *x*, *y*, and *z*-directions according to the global axis tool (Fig. 4). The loading roller is allowed to move only in the z-direction. Loading roller velocity was given as a constant 1 mm/min in the +*z* direction. The number of elements belonging to the simulated finite element model was determined as 43.246 and the number of nodes as 49.522.

3.2. Material model

There are various two-dimensional material models in the LS-DYNA finite element program that describe the damage conditions of composite materials. However, for a three-dimensional examination of the damage conditions of composite plates after a short beam test, the MAT162 material model was preferred. Fiber tensile, fiber crush, matrix, and delamination damages occurring in composite structures are observed progressively with this model, which allows for the definition of the Hashin damage criterion. A total of 34 parameters are needed to define the material model in the MAT162 program. Mechanical properties and damage parameters obtained for the MAT162 material model are given in Table 1 and Table 2, where 1, 2, and 3 represent the axes of composite materials parallel to the fiber, perpendicular to the fiber, and along the thickness, respectively.

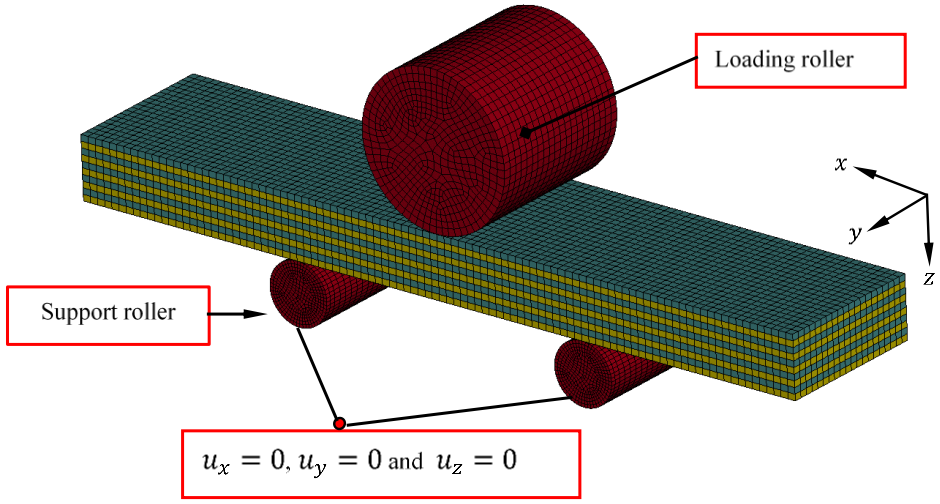

Fig. 4. Numerical model of the short beam test setup

Table 1. Mechanical properties of glass fiber/epoxy composite [13]

Parameter (Unit)	E_1 (GPa)	E_2 (GPa)	E_3 (GPa)	ν_{12}	ν_{23}	ν_{31}	G_{12} (GPa)	G_{23} (GPa)	G_{31} (GPa)
Value	19	19	6	0.162	0.162	0.162	3.786	1.709	1.709
Parameter (Unit)	X_{1t} (GPa)	X_{1c} (GPa)	X_{2t} (GPa)	X_{2c} (GPa)	X_{3t} (GPa)	S_{12} (GPa)	S_{23} (GPa)	S_{31} (GPa)	ρ (kg/m3)
Value	0.459	0.2238	0.459	0.2238	0.0459	0.0828	0.09023	0.09023	1681.39

Table 2. Damage properties of glass fiber/epoxy composite [13]

Parameter (Unit)	SFC (GPa)	SFS (GPa)	AM_1	AM_2	AM_3	AM_4	SFFC	Create 1
Value	0.358	0.118	0.05	0.05	8	-0.2	0.3	0.0449
Parameter (Unit)	Create 2	Create 3	Create 4	SDELM	OMGMX	E_LIMT	EEXPN	φ (°)
Value	0.0339	0	0.0477	1.2	0.999	1.1	1.1	10

3.3. Damage mechanism of composite

MAT162 material model is based on Hashin's [14] principle of progressive damage and the damage mechanics of Matzenmiller et al. [15]. This material model is used to model the progressive damage caused on unidirectional and woven fabric layers subjected to a high shape change ratio and high-pressure loading conditions. In the progressive damage model, the onset of damage is governed by equations. Equations of different types of damage are given below as Equations 4-11. Here, when damage thresholds (r_7, r_8, r_9, r_{10}, r_{11}, r_{12}, r_{13}) reach a value of 1, the initial damage condition is obtained.

3.3.1. Fiber tensile/shear failure modes

The fill and warp fiber tensile/shear damage is given by the quadratic interaction between the associated axial and thickness-shear strains [16].

$$\left(\frac{E_a.\varepsilon_a}{S_{aT}}\right)^2 + \left(\frac{G_{ac}.\varepsilon_{ac}}{S_{AFS}}\right)^2 - {r_7}^2 = 0 \text{ (in direction } a) \tag{4}$$

$$\left(\frac{E_b.\varepsilon_b}{S_{bT}}\right)^2 + \left(\frac{G_{bc}.\varepsilon_{bc}}{S_{BFS}}\right)^2 - {r_8}^2 = 0 \text{ (in direction } b) \tag{5}$$

where, for the fabric model, a, b, and c denote the in-plane fill, in-plane warp, and out-of-plane directions, respectively. E and G are tensile and shear moduli. S_{aT} and S_{bT} are tensile strengths in the fill and warp directions, S_{AFS} and S_{BFS} are fiber shear failure strengths in ac and bc directions, ε_a and ε_b are tensile strains in a and b directions, ε_{ac} and ε_{bc} are shear strains in $a-c$ and $b-c$ planes, and r_7, r_8 are damage thresholds[16].

3.3.2. Fiber compressive failure mode

It is assumed that the in-plane compressive damage in the fill and warp directions is given by the maximum strain criterion as

$$\left(\frac{E_a.\varepsilon'_a}{S_{aC}}\right)^2 - {r_9}^2 = 0, \quad \varepsilon'_a = -\varepsilon_a - \langle\varepsilon_c\rangle \frac{E_C}{E_a} = 0 \text{ (in direction } a) \tag{6}$$

$$\left(\frac{E_b.\varepsilon'_b}{S_{bC}}\right)^2 - {r_{10}}^2 = 0, \quad \varepsilon'_b = -\varepsilon_b - \langle\varepsilon_c\rangle \frac{E_C}{E_a} = 0 \text{ (in direction } b) \tag{7}$$

where S_{aC} and S_{bC} are in-plane compressive strengths[16].

3.3.3. Fiber crush failure mode

The crush damage due to the high through-thickness compressive pressure is modeled using the following criterion:

$$\left(\frac{E_c.\varepsilon_c}{S_{FC}}\right)^2 - {r_{11}}^2 = 0 \tag{8}$$

where S_{FC} is fiber crush strength[16].

3.3.4. In-plane matrix failure mode

A plain weave layer can be damaged under in-plane shear stress without the occurrence of fiber breakage. The in-plain matrix damage mode is given as,

$$\left(\frac{G_{ab}.\varepsilon_{ab}}{S_{ab}}\right)^2 - {r_{12}}^2 = 0 \tag{9}$$

where S_{ab} is the layer shear strength due to matrix shear failure[16].

3.3.5. Parallel matrix failure mode (delamination)

The interlaminar shear strengths are considered to increase under through-thickness compressive stress and decrease due to through-thickness tensile stress according to the Mohr–Columb theory as

$$S_{SRC} = -\varepsilon_c \, E_c \, \tan\varphi \tag{10}$$

where φ is equivalent to the angle for internal friction and ε_c equals to the through-thickness strain, positive when

$$(S)^2 = \left\{\left(\frac{E_c \langle \varepsilon_c \rangle}{S_{cT}}\right)^2 + \left(\frac{G_{bc} \, . \varepsilon_{bc}}{S_{bc0} + S_{SRC}}\right)^2 + \left(\frac{G_{ca} \, . \varepsilon_{ca}}{S_{ca0} + S_{SRC}}\right)^2\right\} - {r_{13}}^2 = 0 \tag{11}$$

where S_{cT} is through-thickness tensile strength, S_{bc0}, S_{ca0} are interlaminar shear strengths in $a-c$ and $b-c$ planes, respectively. S is the factor to take into account when evaluating the effect of stress concentration on the growth of delamination[16].

3.3.6. Damage progressive criterion

Progressive damage is considered with six damage variables $\bar{\omega}_i$, with $i = 1, \ldots, 6$ which degrade the composite stiffness resulting from damage in the different modes [17]. The damage model proposed by Matzenmiller [4] correlates the compliance matrix $[S]$ with the damage variables, as in Equation. (12).

$$[S] = \begin{bmatrix} \frac{1}{(1-\bar{\omega}_1)E_a} & \frac{-\nu_{ba}}{E_b} & \frac{-\nu_{ca}}{E_c} & 0 & 0 & 0 \\ \frac{-\nu_{ab}}{E_a} & \frac{1}{(1-\bar{\omega}_2)E_b} & \frac{-\nu_{cb}}{E_c} & 0 & 0 & 0 \\ \frac{-\nu_{ac}}{E_a} & \frac{-\nu_{bc}}{E_b} & \frac{1}{(1-\bar{\omega}_3)E_c} & 0 & 0 & 0 \\ 0 & 0 & 0 & \frac{1}{(1-\bar{\omega}_4)G_{ab}} & 0 & 0 \\ 0 & 0 & 0 & 0 & \frac{1}{(1-\bar{\omega}_5)G_{bc}} & 0 \\ 0 & 0 & 0 & 0 & 0 & \frac{1}{(1-\bar{\omega}_6)G_{ca}} \end{bmatrix} \tag{12}$$

A damage coupling matrix associates each failure criterion with the reduction of the specific stiffness properties. The exponential damage evolution law as a function of strain was proposed in MAT162 as shown below:

$$(\bar{\omega}_i) = 1 - \exp\left(\frac{1}{AM}\left(1 - r_j^{AM}\right)\right) \; j = 7, \ldots, 13 \tag{13}$$

where AM represents one of four softening parameters controlling compressive fiber failure mode in a direction (1), the tensile and compressive fiber failure mode in b direction (2), for softening associated with fiber crush mode (3), and the in-plane and out-of-plane matrix failure modes (4). The value considered in this work for the softening parameters as $AM_l \; l = 1, \ldots, 4$ are reported in Table 2. The damage threshold, r_k, in a specific direction, k, can also be defined as

$$r_j = \frac{\varepsilon_k}{\varepsilon_{k-yield}}, k = 1, \ldots, 6 \tag{14}$$

where ε is the strain along the k direction and $\varepsilon_{k-yield}$ is the corresponding yield strain.

4. Results and discussion

Experimental and numerical short-beam tests were carried out to determine the shear resistance between layers in laminated glass fiber composites. The graphs obtained as a result of experiments and numerical analyzes are presented by comparing them.

In Fig. 5, the contact force-displacement graph of the glass fiber composite sample is given experimentally and numerically. It was seen that the results of the analysis were compatible. It has been observed that the slopes are quite close to each other, especially in the elastic region. With the contact, the contact force value read on the loading roller started to increase, and after reaching the maximum point, it was observed that it gradually decreased due to fiber damage in the composite sample. The maximum force value read here is defined as the damage load [2]. The first linear ascending portion of the curve represents the stiffness of the undamaged plate. The second part of the curve shows the phase of unloading with damage [18].

In Fig. 6, the change of contact force depending on time is given. In the first region where a linear increase was observed, it was seen that the curves had similar slopes and the maximum contact forces were close to each other. According to the experimental test results, this value was 3603 N on average, while it was 3290 N in the numerical analysis.

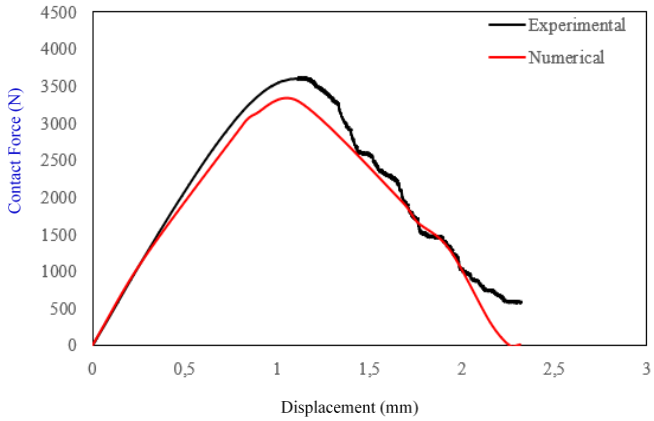

Fig. 5. Contact force-displacement graph

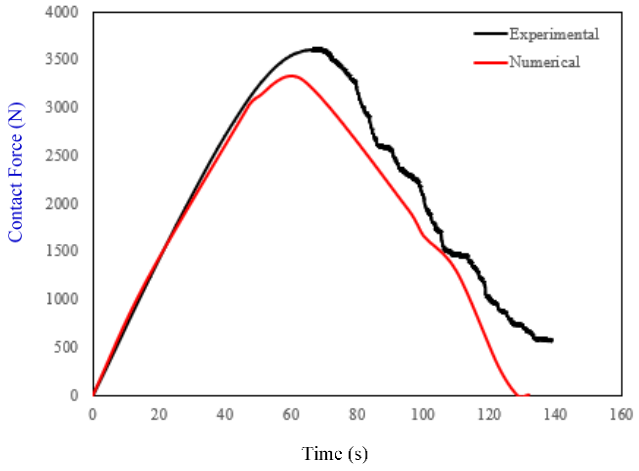

Fig. 6. Contact force-time graph

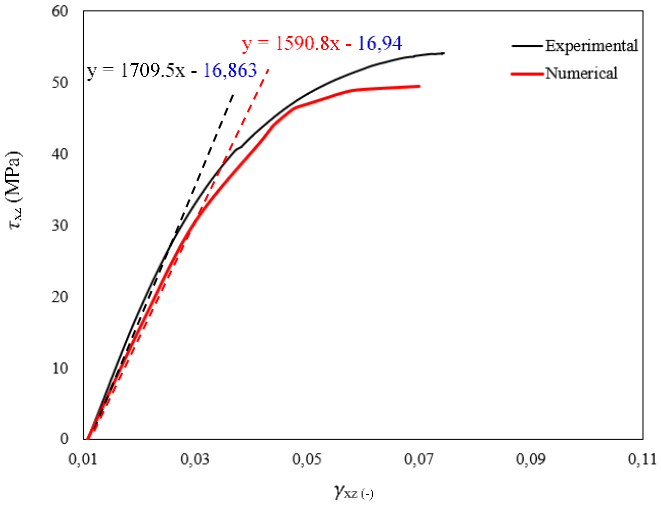

Fig. 7. Shear stress-shear strain graph

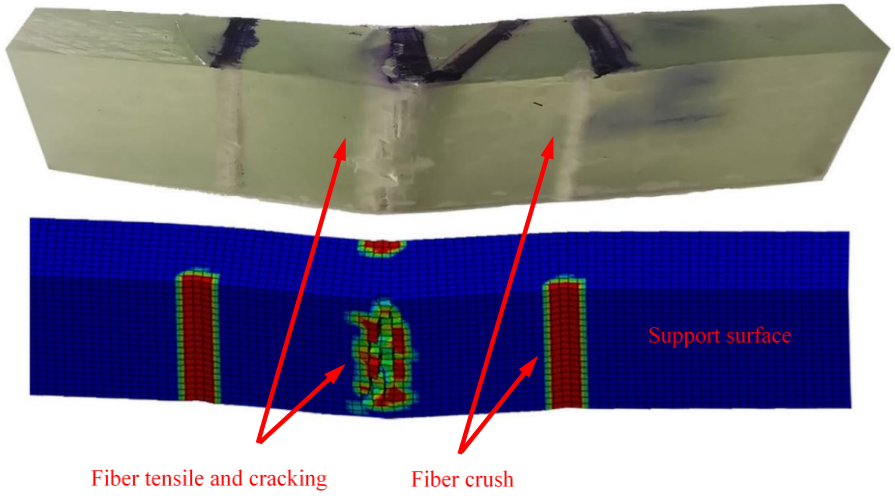

Fig. 8. Experimental and numerical comparison of fiber crack and crush damage

In Fig. 7, the graph of interlaminar shear stress-shear strain is compared experimentally and numerically. The graph also shows the slopes of the ascending curves in the elastic region. These slopes represent the out-plane shear modulus (G_{xz}) of the samples as stated in equation 3. According to the experimental test results, while this value was 1709.5 MPa, it was obtained as 1590.8 MPa in numerical analysis. According to the data obtained, the approximation ratio between the experimental and numerical results was determined as 93%. Gagani et al. [19] performed three-point and four-point bending tests on glass fiber composites. When they compared the maximum shear stresses numerically and experimentally, they achieved a 65 percent agreement. Similarly, the maximum shear strengths between layers were observed experimentally and numerically as 54.05 MPa and 49.5 MPa, respectively.

In Fig. 8, fiber breakage, fiber shrinkage, and fiber crush damage areas in the glass fiber composite sample after the short beam test were compared numerically and experimentally. The surface that the support rollers touch is given as the support surface. When the finite element model is examined, the MAT162 material

model well predicted the fiber breakage, fiber shrinkage, and fiber crush damage regions for the glass fiber composite. It is seen that the experimental and numerical damage areas are generally close to each other.

5. Conclusions

In this study, glass fiber composites were produced by the vacuum infusion method, and by performing a short beam test on the obtained samples, the shear strength and modulus between layers were determined experimentally and numerically. When the results were compared, it was observed that the numerical data were in good agreement with the experimental results. The findings from the tests and numerical simulations are summarized below:

1. When the interlayer shear strength of glass fiber composites was compared experimentally and numerically, it was observed that the experimental results were 93% compatible with the numerical analysis.
2. As a result of the tests and analyzes, the approximation rate of 91% was determined when the interlayer shear modulus was compared.
3. For glass fiber composite, fiber breakage, fiber shrinkage, and fiber crush damage regions were obtained experimentally and numerically.
4. The limitations of this study are; The fiber angles used in the analysis are fixed and 0 degrees. In addition, many material parameters are needed to define the material model for the program, which is challenging for different material types.

Acknowledgments

The authors would like to thank Prof. Dr. Mustafa Güden and Prof. Dr. Alper Taşdemirci from İzmir Institute of Technology, who achieved the Split Hopkinson Bar test to find the "Creates" parameters that use in the MAT-162 model. The authors would also like to thank the Fırat University Scientific Research Coordination Unit, which supported this study with project number MF20.10.

References

[1] Espadas-Escalante JJ, Isaksson P (2019) A study of induced delamination and failure in woven composite laminates subject to short-beam shear testing. Eng Fract Mech 205:359–369. https://doi.org/10.1016/j.engfracmech.2018.10.015

[2] Sritharan R, Askari D (2021) Enhancing the short-beam strength of composite laminates using helical carbon nanotubes. Compos Part B Eng 221:108999. https://doi.org/10.1016/j.compositesb.2021.108999

[3] Allott NR, Czabaj MW (2021) Characterization of the interlaminar shear strength of IM7/8552 using small-scale short beam shear tests. Compos Part A Appl Sci Manuf 142:106200. https://doi.org/10.1016/j.compositesa.2020.106200

[4] Tretiak I, Kawashita LF, Hallett SR (2022) Predicting short beam shear strength reduction in carbon/epoxy laminates containing voids. Compos Struct 290:115472. https://doi.org/10.1016/j.compstruct.2022.115472

[5] Demiral M, Tanabi H, Sabuncuoglu B (2020) Experimental and numerical investigation of transverse shear behavior of glass-fibre composites with embedded vascular channel. Compos Struct 252:112697. https://doi.org/10.1016/j.compstruct.2020.112697

[6] Gupta RK, Mahato A, Bhattacharya A (2021) Damage analysis of carbon fiber reinforced aluminum laminate under short beam and single edge notch beam bend test. Int J Mech Sci 198:106393. https://doi.org/10.1016/j.ijmecsci.2021.106393

[7] Kotik H, Ipiña JP (2015) Influence of Unifilo® Ply in the interlaminar shear fatigue resistance of GFRP. Procedia Mater Sci 8:139–147. https://doi.org/10.1016/j.mspro.2015.04.057

[8] Xin Z, Ma Y, Chen Y, Wang B, Xiao H, Duan Y (2023) Fusion-bonding performance of short and continuous carbon fiber synergistic reinforced composites using fused filament fabrication. Compos Part B Eng 248:110370. https://doi.org/10.1016/j.compositesb.2022.110370

[9] Sai Dinesh K, Gowthaman S (2021) Short beam shear behaviour of ZnO nanowire reinforced glass/epoxy composites. Mater Today Proc 44:821–826. https://doi.org/10.1016/j.matpr.2020.10.713

[10] Kapti S, Sayman O, Ozen M, Benli S (2010) Experimental and numerical failure analysis of carbon/epoxy laminated composite joints under different conditions. Mater Des 31(10):4933–4942. https://doi.org/10.1016/j.matdes.2010.05.018

[11] Shekar KC, Prasad BA, Prasad NE (2014) Interlaminar shear strength of multi-walled carbon nanotube and carbon fiber reinforced, epoxy–matrix hybrid composite. Procedia Mater Sci 6:1336–1343. https://doi.org/10.1016/j.mspro.2014.07.112

[12] Gere J, Goodno, BJ (2008) Mechanics of Materials. 7th ed. Cengage Learning.

[13] Albayrak M, Kaman MO, Bozkurt I (2022) Determination of LS-DYNA MAT162 material input parameters for low-velocity impact analysis of layered composites. Conference Proceedings, Paris, France.

[14] Hashin Z (1980) Failure criteria for unidirectional fiber composites. J Appl Mech Trans ASME 47(2):329–334. https://doi.org/10.1115/1.3153664

[15] Matzenmiller A, Lubliner J, Taylor RL (1995) A constitutive model for anisotropic damage in fiber-composites. Mech Mater 20(2):125–152. https://doi.org/10.1016/0167-6636(94)00053-0

[16] Xiao JR, Gama BA, Gillespie JW (2007) Progressive damage and delamination in plain weave S-2 glass/SC-15 composites under quasi-static punch-shear loading. Compos Struct 78(2):182–196. https://doi.org/10.1016/j.compstruct.2005.09.001

[17] Vescovini A, Balen L, Scazzosi R, da Silva AAX, Amico SC, Giglioa M, Manes A (2021) Numerical investigation on the hybridization effect in inter-ply S2-glass and aramid woven composites subjected to ballistic impacts. Compos Struct 276:114506. https://doi.org/10.1016/j.compstruct.2021.114506

[18] García-Moreno I, Caminero MÁ, Rodríguez GP, López-Cela JJ (2019) Effect of thermal ageing on the impact damage resistance and tolerance of carbon-fibre-reinforced epoxy laminates. Polymers (Basel) 11(1):10–12. https://doi.org/10.3390/polym11010160

[19] Gagani AI, Krauklis AE, Sæter E, Vedvik NP, Echtermeyer AT (2019) A novel method for testing and determining ILSS for marine and offshore composites. Compos Struct 220:431–440. https://doi.org/10.1016/j.compstruct.2019.04.040